Molecular Crystals and Liquid Crystals

ISSN: 1542-1406 (Print) 1563-5287 (Online) Journal homepage: http://www.tandfonline.com/loi/gmcl20

Electro-Optics of Nematic/Gold Nanoparticles Composites: The Effect from Dopants

Georgi B. Hadjichristov, Yordan G. Marinov, Alexander G. Petrov, Emanuela Bruno, Lucia Marino & Nicola Scaramuzza

To cite this article: Georgi B. Hadjichristov, Yordan G. Marinov, Alexander G. Petrov, Emanuela Bruno, Lucia Marino & Nicola Scaramuzza (2015) Electro-Optics of Nematic/Gold Nanoparticles Composites: The Effect from Dopants, Molecular Crystals and Liquid Crystals, 610:1, 135-148, DOI: 10.1080/15421406.2015.1025619

To link to this article: http://dx.doi.org/10.1080/15421406.2015.1025619

Published online: 06 Jul 2015.

Mol. Cryst. Liq. Cryst., Vol. 610: pp. 135–148, 2015

ISSN: 1542-1406 print/1563-5287 online
DOI: 10.1080/15421406.2015.1025619

Taylor & Francis
Taylor & Francis Group

Electro-Optics of Nematic/Gold Nanoparticles Composites: The Effect from Dopants

GEORGI B. HADJICHRISTOV,[1,*] YORDAN G. MARINOV,[1] ALEXANDER G. PETROV,[1] EMANUELA BRUNO,[2] LUCIA MARINO,[3] AND NICOLA SCARAMUZZA[2,3]

[1]Institute of Solid State Physics, Bulgarian Academy of Sciences, Sofia, Bulgaria
[2]Dipartimento di Fisica, Università della Calabria, Rende (CS), Italy
[3]CNR-IPCF UoS di Cosenza, Licryl Laboratory, and Centro di Eccellenza CEMIF.CAL, Università della Calabria, Rende (CS), Italy

We studied the change of electro-optic properties of room-temperature nematic pentylcyanobiphenyl (5CB) when this liquid crystal is mixed with a small amount (∼ 0.5 wt.%) of polymer-capped gold nanoparticles (AuNPs). The AuNPs were spherical-shaped, with a diameter of about 12 nm, the size of the polymer-capped AuNPs was ca. 25 nm. Instead of well pronounced stationary longitudinal domains observed in planar 5CB nematic layers upon static electric field, hybrid longitudinal texture pattern oriented along the rubbing of the cells takes place in this case in identical cells of 5CB doped with AuNPs. The micro-periodic-modulated morphology is reflected on the electro-optic response of AuNPs/5CB nanocomposites. The effect from the nano-dopants is elucidated by detailed investigation (optical, thermo-optical, electrical and electro-optical macroscopic measurements).

Keywords nanostructured liquid crystals; gold nanoparticles; nematic nanocomposites; nanomaterials; electro-optics; coherent light scattering

1. Introduction

In recent years, the novel liquid crystal (LC) nanocomposites have attracted a great scientific and technological interest due to their promising practical applications, like displays, flat-panels, innovative sensors and digital non-volatile memory devices [1–11]. In this context, the nanoparticle (NP) doping of LCs has been actively studied for enhancing LC properties for advanced applications, since this process is easier than other methods and is conventionally applicable. Nanostructured materials from gold NPs (AuNPs) dispersed in proper LCs have found an increasingly important area of research because of the unique combination of LCs and NPs that can be controlled by electric fields [12–19]. In particular, LC nanocomposites with polymer-capped AuNPs have been investigated toward the realization of nonvolatile memory for electronic storage devices [20].

*Address correspondence to Georgi B. Hadjichristov, Institute of Solid State Physics, Bulgarian Academy of Sciences, 72 Tzarigradsko Chaussee Blvd., BG-1784 Sofia, Bulgaria. E-mail: georgibh@issp.bas.bg

Color versions of one or more of the figures in the article can be found online at www.tandfonline.com/gmcl.

Very recently, we have reported on the scatter-based electro-optical (EO) response of thin films composed of room-temperature nematic LC 4-*n*-pentyl-4′-cyanobiphenyl (5CB) doped with 0.5 wt.% polymer-capped AuNPs [21]. The electro-optics of AuNPs/5CB nanocomposite in planar cells was linked to the corresponding electric field-induced textural changes. The presented work aims to clarify the effect of the AuNPs dopants, how they actually change the host nematic 5CB resulting in a strong reduction of coherent light transmittance of initially planar AuNPs/5CB nanocomposite films under low-voltage static electric field.

2. Experimental

The preparation of the polymer-capped gold nanoparticles (AuNPs) used here has been described in detail elsewhere [20]. The uncoated AuNPs were highly monodisperse and quasispherical with a mean diameter of ca. 12 nm, as estimated by SEM. The diameter of the polymer-coated particles was about 25 nm. Mixture from the capped AuNPs at concentration 0.5 wt.% in the LC 5CB (from Merck) was prepared as described in [21]. Using capillary suction, the AuNPs/5CB mixture was spread into a planar aligned polyimide-coated commercial KSRO-25/B111N1NSS Up/Low glass cells (EHC Ltd, Tokyo, Japan) with a thickness of (25 ± 0.2) μm and an ITO resistance of 100 $\Omega\ \square^{-1}$. The formation of the nematic LC phase was examined with polarizing microscope by observing birefringence between crossed polarizers. The unidirectionally rubbed polyimide provided a strong planar alignment of the LC having an overall orientation of the director along the rubbing direction.

The morphology changes of the prepared films by electric field were characterized by transmission optical microscopy (Zeiss Axioskop polarizing microscope). The microscope images were recorded by a Cannon EOS 7D video camera and computer. Voltage-dependent coherent light transmittance of the films was measured by use of the beam of a linearly polarized He-Ne laser Melles Griot 05-LHP-201 (10 mW)). The incident laser beam (wavelength $\lambda = 632.8$ nm) with diameter of about 1 mm was directed normally to the LC film plane (more correctly, nearly normally, to avoid the optical interference by reflections from optical elements). The laser power incident on the LC cells was $\sim$1 mW.

Electric field was applied across the two indium-tin-oxide (ITO) coated slides of the LC cell (i.e. the electric field direction coincides with the laser beam direction). The light transmitted through the LC cells was detected by photodiode placed at a distance of 90 cm to the cell. The light intensity was measured with a computer-controlled system with automated data acquirement. Direct current (DC) or alternating current (AC) (sinusoidal) voltages were supplied by HP 8904A Multifunction Synthesizer DC-600kHz interfaced with HP 34401A Multimeter. The transmittance of the cells was recorded in steps of 0.1 V and 0.01 V as a function of DC voltage and AC voltage, respectively. The interval between the data acquirement was equal to 30 s, an averaging of 10 measurements was done during 10 s at each step. During the voltage sweep, the stationary state of the nematic in the cells was permanently controlled by oscilloscope

For response time measurement, the photodiode output was acquired by Agilent Infiniium 54832D MSO digital storage oscilloscope. For thermo-optical experiments, the temperature of the studied cells was controlled (with an accuracy of $\pm$ 0.1°C) by a hot stage (Mettler FP82). The optical transmittance of the LC cells in the wavelength range of 300–800 nm was measured by means of Varian Cary 5E UV-Vis-NIR Spectrophotometer. The spectra were recorded with a spectral resolution of 1 nm.

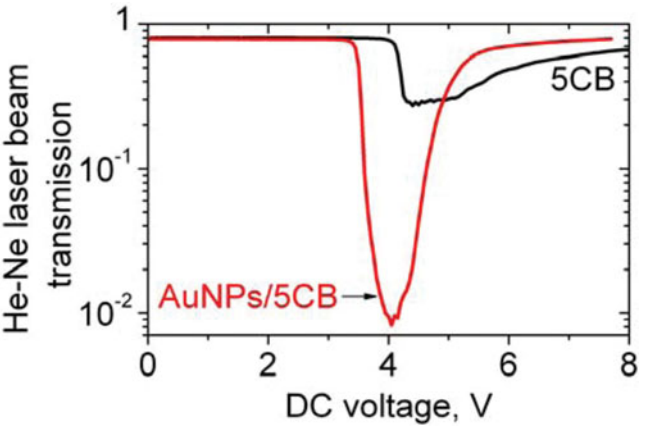

Figure 1. Comparison of the DC voltage-dependent light transmittance of AuNPs/5CB composite and that of pure 5CB in identical planar cells (25 μm-thick). Both transmittance curves were measured under identical experimental conditions. Far-field laser beam intensity change was detected. The polarization of the probe He-Ne laser beam was parallel to the rubbing of the cells. The temperature of the cells was 28°C.

The current-voltage characteristics of the examined cells were obtained by a voltage sweep at intervals of 30 s. DC electrical measurements were conducted by Keithley 617 Programmable Electrometer controlled by computer. The measurement accuracy in this case was ± 0.05% and ± (0.15%–0.25%) for the values of the voltage and the current, respectively. AC measurements were carried out by computer-controlled lock-in amplifier (SR830, Stanford Research Systems). A sinusoidal voltage from the lock-in instrument was applied to the ITO electrodes of the cells (and can be optionally mixed with a driving DC voltage). By EO modulation measurements, the photodiode signal was acquired by the lock-in instrument and then by a computer that controls the frequency sweep (in the range from 1 Hz to 30 kHz).

3. Results and Discussion

By prepared planar cells with AuNPs/5CB, a strong reduction of the coherent light transmittance was observed upon a low-voltage static electric field (Figure 1). In this case, the EO response of the composite films was probed by a laser beam ($\lambda = 632.8$ nm) whose linear polarization was parallel to the rubbing of the cells. After a well pronounced threshold at the DC voltage (V_{DC}) = 3.2–3.3 V, further increase of V_{DC} led to a sharp decrease of the transmitted light intensity. As indicated our tests, this is due to coherent light scattering (LS) from the stationary spatially-modulated quasi-regular longitudinal narrow-striped domain texture formed in our planar cells with nanocomposite nematic [21]. The process of coherent LS is competed by coherent light diffraction. The two mechanisms could be hardly separated and distinct voltage regions corresponding to each mechanism (separate) can not be exactly specified.

As a result from both optical coherent processes (coherent light scattering and diffraction) and electrically-driven nematic director reorientation, the initially planar AuNPs/5CB films exhibit characteristic V-shaped curves (sharp and narrow) of V_{DC}-controlled coherent light transmittance. As seen in Figure 1, the laser beam intensity reduction effect is also

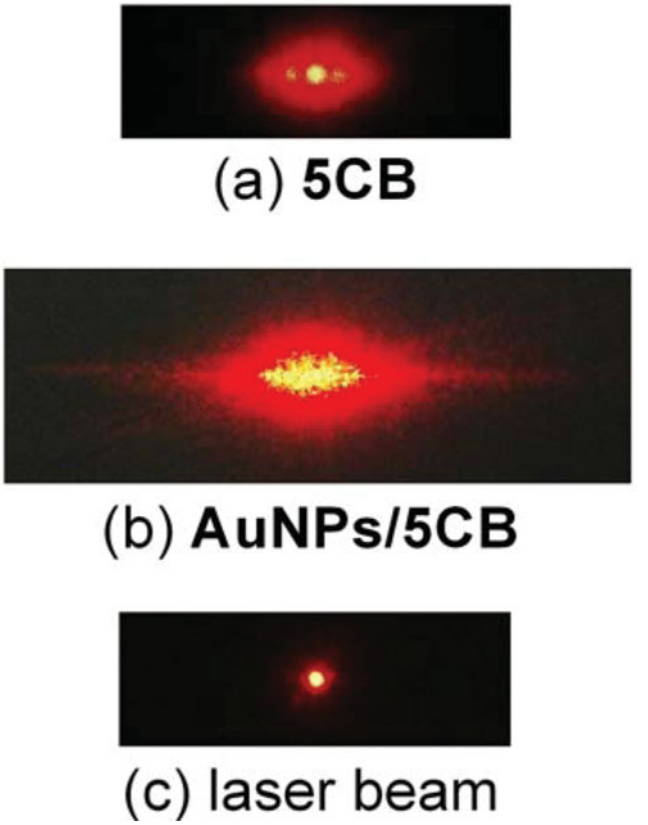

Figure 2. Diffraction/scattering patterns as visually observed on a transversal imaging screen by transmission of He-Ne laser beam through identical planar cells (thickness 25 μm) with: (a) 5CB; (b) AuNPs/5CB composite, both at DC voltage of 4.5 V. In both cases, the polarization of the incident laser beam was along the direction of the rubbing of the cells; the other experimental conditions are also the same, the temperature was 29°C; (c) - the beam shape corresponding in both cases to the transmission at zero field, given for comparison.

present for pure 5CB in identical planar cells, but its degree is much lower than the one for AuNPs/5CB composites. By 5CB planar cells, spatially resolved diffraction orders can be clearly viewed (Figure 2 (a)) within a certain V_{DC} range (in our case, 4.3 V – 7 V), in contrast to the largely spread coherent LS observed by composite AuNPs/5CB films (Figure 2(b)). No change of the transmitted laser beam takes place when the beam polarization orientation is orthogonal to the rubbing of the cell plates.

Optical microscopy clearly indicated the morphology difference between the two nematic LC materials, 5CB and doped 5CB, in identical planar cells, viewed upon DC voltage in the range from 0 to 10 V. For doped 5CB (Figure 3(b), it is seen the lack of V_{DC}-induced wide-formed longitudinal domains (LDs) present in initially planarly-aligned 5CB layers (Figure 3(a)) subjected to the same DC voltage. The wide-formed texture pattern oriented along the rubbing direction has a flexoelectric nature, like the flexodomains long known for nematic LC compounds upon DC (or very low-frequency alternating-current) electric field [22–26]. In particular, similar wide-formed LDs in 5CB planar cells subjected to the combined action of DC and AC electric fields was thoroughly investigated [27]. In

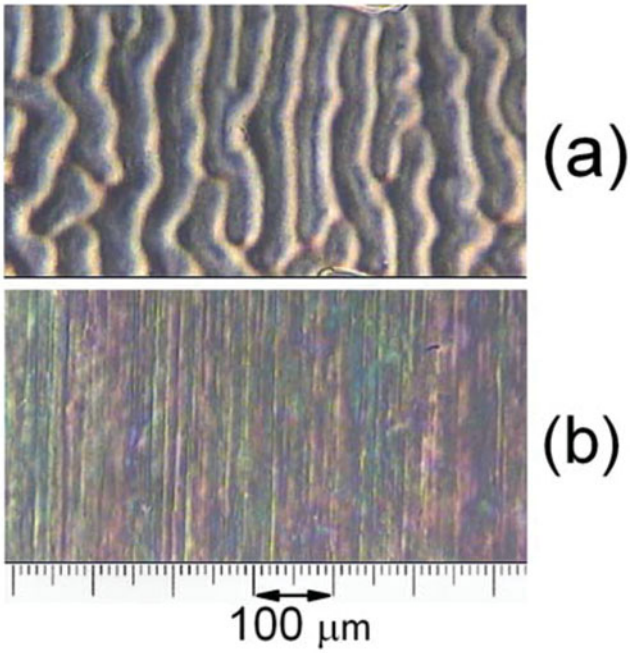

Figure 3. Polarizing microscopy pictures for pure 5CB (a) and 5CB doped with AuNPs (b) in identical planar cells (25 μm-thick). The micrographs were taken by slightly uncrossed polarizers, the input light polarization was parallel to the rubbing of the cells. In both cases, the applied DC voltage was 4.5 V, the temperature was 29°C.

our case, these stationary nearly regular LDs (their detailed description will be published elsewhere) do form a diffraction grating in the plane of the film. Actually, this periodic texture formation leads to a diffraction splitting of the transmitted laser beam in spatially resolved diffraction orders, clearly observed behind the 5CB planar cells at suitable DC voltage (recall Figure 2(a)). The refractive index of the nematic in the grating domains follows the field-driven reorientation of the nematic director.

Instead of wide-formed LDs, a densely spaced longitudinal narrow-formed micro-periodic director modulation texture is present for the AuNPs doped 5CB nematic (Figure 3(b)). These fine (micrometer wide) quasi-regular parallel stripes are also stationary, closely follow the rubbing of the cell plates and can be ascribed to rubbing-induced texture pattern [28]. A detailed inspection of the micrographs taken for the nano-doped 5CB reveals that the wide-formed field-induced LD texture is still present in the apparent narrow-formed longitudinal texture in Figure 3(b). Being latent and sporadic, discernible by microscope mostly at $V_{DC} > 4.2$ V – 4.3 V, the wide-formed LD texture of our AuNPs/5CB planar cells looks like as somewhat 'suppressed'. In fact, the narrow-formed parallel stripes are predominating in such a hybrid texture. Note, the longitudinal texture patterns formed in the cells were observable until the enhancement of hydrodynamic processes (well pronounced at $V_{\mathrm{DC}} > 7$ V) that lead to pattern deformation and destroying. Also, the longitudinal texture formed by DC electric field is erased by AC field (with suitable amplitude) simultaneously applied on the cells (well known quenching effect due to LC reorientation by AC field, reported for static longitudinal domain structures formed upon DC field in 5CB [27] and in other nematics in planar cells [23, 24].

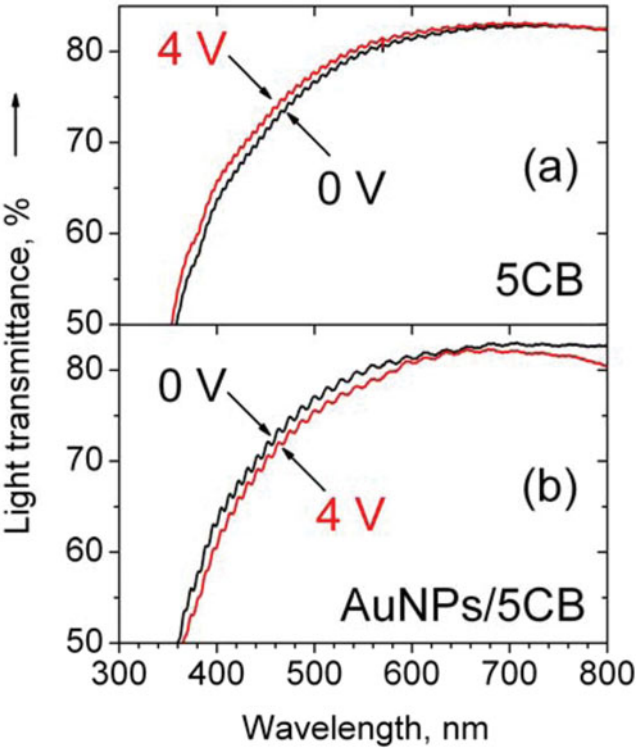

Figure 4. Transmittance spectra of pure 5CB nematic (a) and AuNPs/5CB composite (b) in identical planar cells (25 μm-thick). Data measured by spectrophotometry at DC voltage $V_{DC} = 0$ and $V_{DC} =$ 4 V with unpolarized light under the same other experimental conditions. The temperature was 29°C. The fine oscillations in the curves are due to the known optical interference from the cell plates.

In order to specify the impact of the AuNPs dopants on the 5CB nematic, that leads to the observed light transmittance reduction effect, complementary electro-optical and electrical measurements were performed. At first, the change of the host 5CB due to the presence of AuNPs was clearly evidenced by measurements of DC electric filed-induced change in optical transmittance. Figure 4 compares the transmittance spectra (specular transmission of unpolarized non-coherent light as recorded by spectrophotometry) of 5CB and composite AuNPs/5CB in identical planar cells and, actually, their change upon application of $V_{DC} = 4$ V on the cells. This DC voltage corresponds to the maximum reducing effect for AuNPs/5CB as follows from Figure 1. In contrast to the strong EO effect observed in the AuNPs/5CB probed by far-field laser beam intensity change (a change with at least two orders of magnitude, see Figure 1), a rather weak decrease of 1 – 2% was present in this case for the DC voltage-induced transmittance of the same nanocomposite film measured by photometry (Figure 4(b)). The reduction effect was small, but outside the experimental uncertainty. On the other hand, within the sensitivity limits of our spectral apparatus no such EO effect was observed for the 5CB cells. In the latter case (Figure 4(a)), a slight increase of the film transmittance was detected, reasonably because of the electric filed-driven reorientation of the LC molecules. At the zero voltage, the transmittance of both 5CB and AuNPs/5CB was the same. Indeed, a change of anisotropy of the LC refractive

index in the nematic by the dissolved spherically symmetric AuNPs that are isotropically surrounded by LC molecules, is unlikely.

The mechanism responsible for reduction of the transmitted light by AuNPs/5CB nanocomposites upon DC electric field, is the LS due to field-induced anisotropy of the refractive index of the nematic [21]. The enhanced LS by AuNPs/5CB suggests that the AuNPs dopants introduce disorder in the LC (locally, in the nanoscale vicinity of each nanoparticle), or change the anisotropy properties of the nematic. Note that the scattering is not by NPs themselves as scattering and/or diffractive centers. By polarized transmittance spectra, the difference between the transmittance of the AuNPs/5CB composite at the voltages $V_{DC} = 0$ and $V_{DC} = 4$ V becomes larger. The difference was maximum (ca. 3%) in the case when the polarization axis of the polarizer was parallel to the rubbing of the cell (Figure 5(b)), and negligible at the perpendicular configuration (Figure 5(c)). This agrees with our results obtained by measurement of transmitted laser beam intensity as a function of the polarization direction of the laser beam: the effect of reduction of the transmitted laser beam intensity by coherent LS produced by external DC electric field was strongest when the polarization of the incident laser beam is parallel to the initial orientation of the nematic director and gradually diminishes when the laser beam polarization is rotated towards to the orthogonal one. Note the absence of interference fringes in the spectrum recorded at parallel polarization configuration for the planar cell with doped 5CB subjected to a static electric field (Figure 5(b)). This indicates an unbalance of interfering waves and a strongly reduced modulation (practically nullification) of the resulting optical field. The reason is namely the field-induced LS.

The difference between the considered EO response of planar layers containing the examined mixture of AuNPs and 5CB, and identical cells of pure 5CB under the same experimental conditions and by the given polarization arrangement, is that the LS prevails by the composites. Obviously, AuNPs in the LC enhance the LS (this occurs through the formed micro-periodic director modulation textures, being spatial patterns of optical phase shift, and thereby effective diffractive/scatter structures). By AuNPs/5CB planar cells, the LS can reach its full extent prior to the LS reduction owing to the director reorientation along the external electric field applied on the cells. In fact, this leads to a full minimization of the intensity of the laser beam transmitted through planar cells with AuNPs/5CB composite. The latter operate like EO diffusers. On the contrary, in the pure 5CB cells the strong diffraction with significant zero-order intensity due to the electrically-formed regular wide LDs does not allow the strong reduction of the central intensity of transmitted laser beam. Thus, by eliminating the wide LDs that otherwise should be formed within the planarly-aligned 5CB nematic, AuNPs do enhance the LS. It should be noted that the V-shaped behavior was not present for the same mixture but filled in homeotropic cells. In fact, in this case we did not observed striped longitudinal domains within DC voltage range up to 10 V.

The effect of the AuNPs dopants on the host 5CB nematic where they were mixed was further ascertained by frequency-modulation EO spectroscopy. Figure 6 compares the frequency-modulation EO response (the frequency spectrum for the first harmonic of transmitted laser light modulation measured by lock-in instrument) of both 5CB and AuNPs/5CB subjected to various DC voltages. As seen in Figure 6(a), a peculiarity (a decreasing of the modulation amplitude) is present for the doped 5CB at the DC voltage value ($V_{DC} = 4$ V) corresponding to the minimum of the V-shaped behavior in Figure 1. No such behavioral feature (being a deviation from the common trend) was registered for the frequency-dependent first harmonic signal from pure 5CB (Figure 6(b)). Thus, this

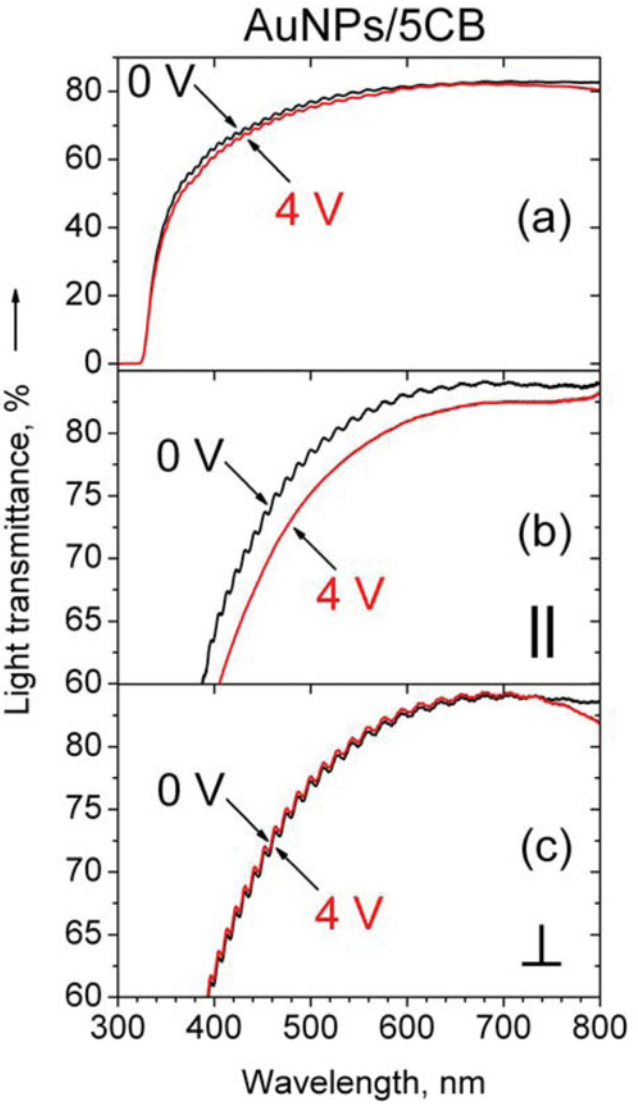

Figure 5. Transmittance spectra of a planar cell with AuNPs/5CB composite (25 μm-thick) at DC voltage $V_{DC} = 0$ and $V_{DC} = 4$ V as measured by spectrophotometry with unpolarized light (a) and light polarized parallel (b) or perpendicular (c) to the rubbing of the cell. The other experimental conditions were kept the same, the temperature was 29°C. The spectra in (b) and (c) were normalized by the spectral response of the polarizer mounted in the spectrometer.

sensitive probe at the macro-level also detects the V_{DC}-induced LS by 5CB nematic in the presence of nano-dopants when efficient scattering textures are formed.

Figure 7 presents the temperature-dependent laser beam transmittance measured for AuNPs/5CB composite and the pure 5CB LC in identical cells. These plots demonstrate that the nematic-to-isotropic (N-I) phase transition temperature of the mixture was higher (by 0.43°C) than that for the pure 5CB. This result was well reproducible and agrees very well with the value (0.4°C) of the temperature shift reported for AuNPs/5CB composites

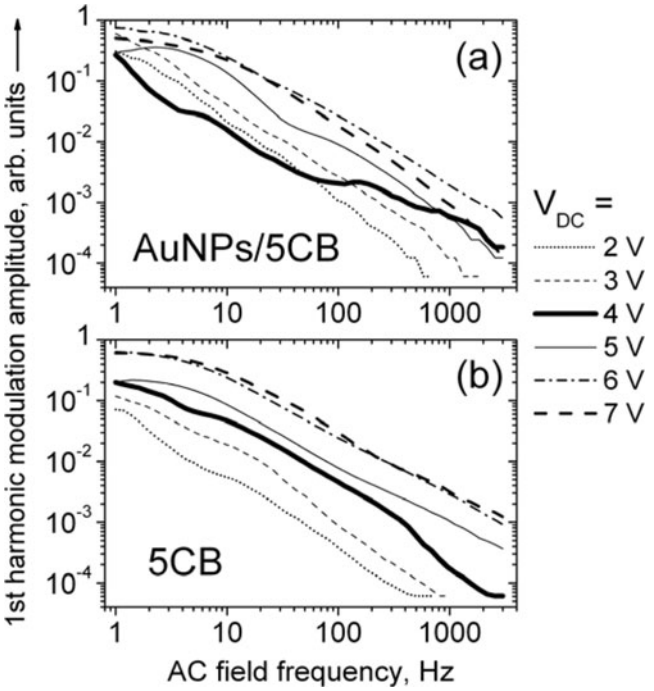

Figure 6. The amplitude of the 1st harmonic of transmitted He-Ne laser light modulation versus the electric-field frequency for AuNPs/5CB (a) and 5CB (b) in identical planar cells as measured by applying various DC voltages (indicated in the graphs) on the cells. The voltage amplitude of the AC electric field was 1 V_{RMS}, the polarization of the probe He-Ne laser beam was parallel to the rubbing of the cells, the temperature of the cells was 23°C.

(AuNPs at concentration of 0.2 wt.%) by Khatua et al [14]. An increase of N-I temperature due to the dispersion of AuNPs in 5CB has been reported also by other researchers (e.g., [17–19]). Contrary to the disorder effect expected for symmetric inclusion of the AuNPs dopants in 5CB, the higher N-I temperature of the doped 5CB points to a nematic order stabilization, but the understanding of the mechanism of the shift of the clearing temperature by polymer-capped AuNPs dopants requires further studies. Most probably, these dopants induce large local electric fields [29, 30] that affect the LC molecules orientation and increase the intermolecular interaction. The increased interaction could possibly contribute to the higher N-I temperature.

A clear change in the properties of the host 5CB resulting from the mixing of this nematic LC with the AuNPs we have employed, was registered by time response measurements under switching the DC voltage on and off (at switching voltage value V_{DC} corresponding to the minimum of the V-shaped behavior given in Figure 1). As seen in Figure 8, by switching the stress voltage V_{DC} on, the relaxation time by the AuNPs/5CB composite is considerably shorter (more than 5 times) than that for the pure 5CB. In contrast, after the switching the DC voltage off, the relaxation time for AuNPs/5CB for recovery of the initial state is about three times larger than that for 5CB (Figure 8(b)). The first observation implies: (i) a reduction of the LC elastic properties by AuNPs dopants; and /or (ii) an enhancement in the dielectric anisotropy of the nano-doped LC; and/or (iii) possible increase of the effective electric field in the doped system. The result for switch-off times

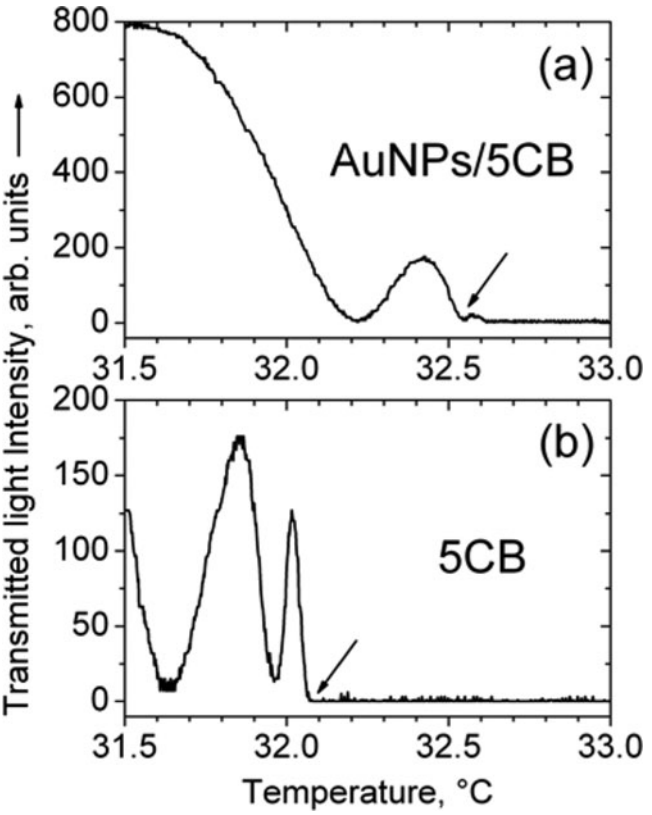

Figure 7. Temperature-dependent transmittance of light ($\lambda = 632.8$ nm) for AuNPs/5CB composite (a) and pure 5CB (b). The measurements were done under the same experimental conditions in identical cells (planar, thickness of 25 μm) placed between crossed polarizers. The incident laser beam polarization at 45° to the rubbing of the cells. The arrows indicate the clearing temperatures in both cases.

is consistent with (i) and (ii). Both effects (i) and (ii) are expected (generally, they are relevant to the structural disorder due to nanoparticles). A complementary measurement of the Fréedericksz transition (Figure 9) reveals a lower threshold voltage by the AuNPs/5CB composite (0.88 V) than for the pure 5CB (0.96 V). The decrease of the threshold voltage we have registered agrees well with data reported for mixtures of AuNPs in 5CB (0.2 wt.% AuNPs) [14]. Various studies indicated that the threshold voltage is reduced by doping of AuNPs into 5CB [17, 18]. The decreased threshold confirms the disorder in the composite (as well as the eventual enhancement in the dielectric anisotropy of the LC that also should result in a lower threshold voltage). Correlated with the contraindicative increase in the N-I temperature by AuNPs/5CB discussed above, one can consider the factor (ii) as the most likely explanation for the observed threshold decrease, as pointed out by Khatua et al [14]. However, the decreasing threshold found for AuNPs/5CB is also indicative of possible impact of the factor (iii) owing to NP-doping of 5CB, which in our case needs a further experimental proof (given below).

Very indicative of the change of the hosting 5CB nematic by the doped polymer-capped AuNPs are the current-voltage characteristics of the cells. As seen from Figure 10, above

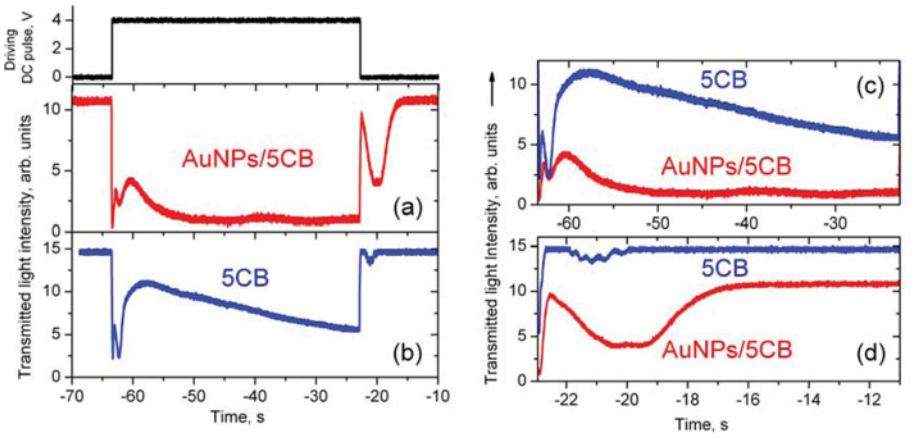

Figure 8. Time response of the AuNPs/5CB composite (a) and pure 5CB (b) measured when a stress DC voltage of 4 V applied on identical planar cells with both materials is switched on and off (the pulse is shown at the top). The experimental conditions are kept the same in both cases. The polarization of the probe He-Ne laser beam was along to the rubbing of the cells. The temperature was 28°C. (c,d) – as (a,b), but showing the expanded fronts: the rising wings (c) and the falling tails (d).

a certain threshold voltage, in our case near 4 V (Figure 10(a)), the DC conductivity of AuNPs/5CB is lower than that of 5CB itself, in contrast to the significant increase of the ionic conductivity in the case of composites of uncoated AuNPs with 5CB (compared again to that of the pure 5CB sample) [12, 17]. Note, this value is near to the formation threshold

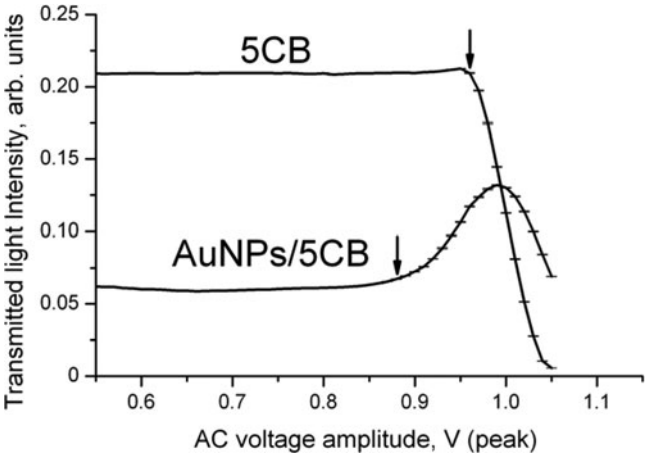

Figure 9. EO response of AuNPs/5CB composite and pure 5CB in identical planar cells (planar, thickness of 25 μm) placed between crossed polarizers. Light transmittance was measured vs the voltage of AC field at frequency of 1 kHz applied on the cells. The experimental conditions are kept the same in both cases (voltage step = 0.01 V; interval between the measured data = 10 s; 10 averaging). The probe He-Ne laser beam polarization at 45° to the rubbing of the cells, the temperature fixed at 28°C. The error bars correspond to the standard deviation of the measured data. The arrows represent the threshold voltages.

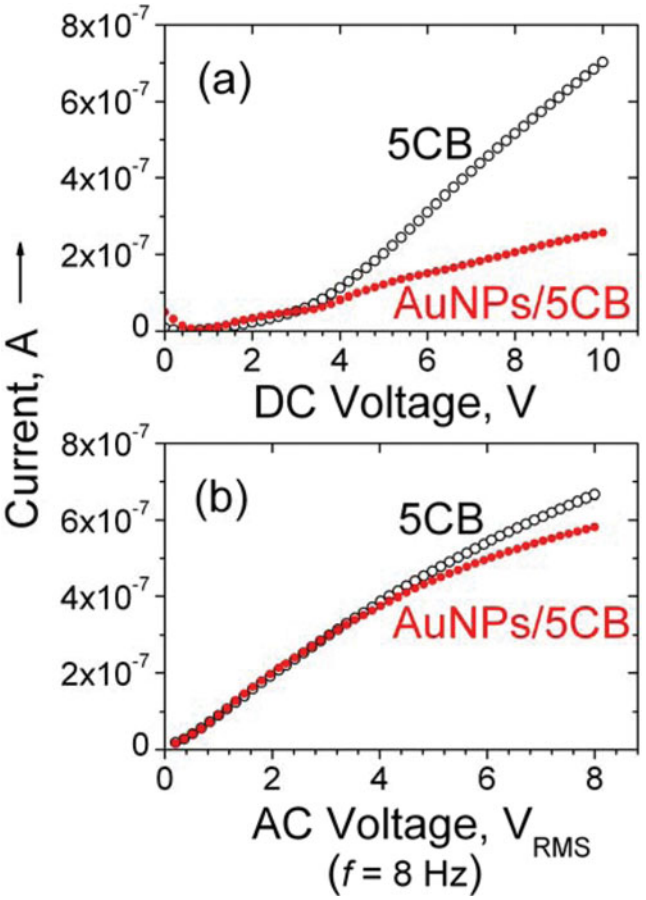

Figure 10. DC (a) and AC (b) current-voltage dependences measured for identical planar cells (25 μm-thick) with pure 5CB nematic and AuNPs/5CB composite, both cells under identical experimental conditions. The temperature of the cells was 29°C.

for the wide LDs mentioned above. The observed behavior (steep when V_{DC} is above a threshold) is in qualitative agreement with results reported in [27] for 5CB planar cells in the case of a pure DC driving. Measured upon AC field at a low-frequency (8 Hz in our experiment), above the almost the same voltage value the AC conductivity of AuNPs/5CB cells becomes lower than that of the reference 5CB cells (Figure 10(b)).

The lower conductivity of the NP-doped system than that of the host 5CB might originate in electric field-induced charge transfer effect from the LC molecules to the AuNPs dopants. The polymer coating of the metal nanospheres enhances this process since the capping acts as an ionic charge trapper [20]. Upon static electric field externally applied on the cells with doped 5CB, the polymer layer capping the AuNPs surface captures ions that induce a space-charge field that opposes to the external field thus reducing the current into the cell. In our case, namely this internal field in the doped 5CB system hinders the development of the wide LDs that otherwise should be created in 5CB nematic in the same planar cells under the same static electric field. Similarly to carbon nanomaterials in nematics upon DC voltage [31, 32]), the gold nanospheres doped in 5CB attract and

capture some free ions in the nematic, this leads to ion depletion, the electric field in the LC system becomes more homogeneous and the gradient flexoeffect is reduced. Due to captured ions and the decreasing screening field in the nano-doped 5CB, the effective electric field is higher than that in 5CB itself. This leads to the above mentioned shortening of the switching-on time measured for AuNPs/5CB as compared to the pure 5CB.

4. Conclusion

The role of the polymer-capped gold spherical nanoparticles (AuNPs) dispersed in the nematic LC 5CB for the extremely enhanced coherent light scattering and thereby, the strong reducing effect observed for the DC voltage-dependent laser beam transmittance of 5CB doped with 0.5 wt.% AuNPs, is clarified. Our experimental evidences clearly indicate that the AuNPs introduce a nano-disorder in 5CB nematic and prohibit the formation of stationary flexodomains due to ion depletion. The latter weakens the flexo-deformations, and thereby stationary flexodomains LDs cannot be developed in AuNPs/5CB nanocomposite planar cells under static electric field.

The different EO response of identical planar cells with both nematic materials considered here (5CB and 0.5 wt.% AuNPs/5CB nanocomposite) is based on their different texture and its electrically-induced change. Thus, regular wide LDs along the rubbing of the cells are formed in the cells with 5CB above a threshold voltage, whereas in the cells with the AuNPs/5CB composite were observed much narrower longitudinal texture stripes that determine the electro-optics of the LC nanocomposite material. Nano-doped nematics with hybrid textures like the one observed here (forming a set of two simultaneous diffraction gratings of wide LDs and narrow longitudinal stripes) can be considered as prospective materials for electrically-switchable/controllable diffractive and adaptive optics.

Similar electro-optical effects based on NP-doping will allow to adopt the nematic nanocomposites for various kinds of photonic applications. Reasonably, for the appearance of strong and electrically-controllable effect (as the EO scattering by AuNPs/5CB nematic nanocomposites in planar cells considered here) of great importance is the structure and the properties of the host LC, as well as the complex balance between hydrodynamic, dielectric and elastic torques. Measurements with other nematic nanocomposites by varying the NP-doping should be made to search and assess similar efficient scatter-based effects (work in progress).

Acknowledgments

INERA EU project Research Potential (FP7-316309-REGPOT-2012-2013-1) “Research and Innovation Capacity Strengthening of ISSP-BAS in Multifunctional Nanostructures” is acknowledged. The authors would like to thank Assoc. Prof. DSc. Hristo Hinov from ISSP-BAS for his valuable comments and suggestions, and for helpful discussions. Funding Work supported by research project DFNI-TO2/18 by the Ministry of Education and Science, National Science Fund of Bulgaria.

References

[1] Garbovskiy, Y. A., & Glushchenko, A. V. (2010). *Solid State Phys*., *62*, 1.
[2] Hinojosa, A., & Sharma, S. C. (2010). *Appl. Phys. Lett.*, *97*, 081114.
[3] Qi, H., & Hegmann, T. (2011). *Liq. Cryst. Today*, *20*, 102.
[4] Jamil, M., Ahmad, F., Rhee, J. T., & Jeon, Y. J. (2011). *Curr. Sci.*, *101*, 1544.

[5] Li, J., Ma, Y., Gu, Y., Khoo, I. C., & Gong, Q. (2011). *Appl. Phys. Lett.*, *98*, 213101.
[6] Shivakumar, U., Mirzaei. J., Feng, X., Sharma, A., Moreira, P., & Hegmann, T. (2011). *Liq. Cryst.*, *38*, 1495.
[7] Ouksova, E., Lysenko, D., Ksondzyk, S., Cseh, L., Mehl, G. H., Reshetnyak, V., & Reznikov, Y. (2011). *Mol. Cryst. Liq. Cryst.*, *545*, 1347.
[8] Lapanik, A., Rudzki, A., Kinkead, B., Qi, H., Hegmann, T., & Haase, W. (2012). *Soft Matter*, *8*, 8722.
[9] Ha, Y. S., Kim, H. J., Park, H. G., & Seo, D. S. (2012). *Opt. Express*, *20*, 6448.
[10] Hegmann, T., Qi, H., & Marx, V. M. (2007). *J. Inorg. Organomet. Polym. Mater.*, *17*, 483.
[11] Xue, C., & Li, Q. (2014). In: *Nanoscience with Liquid Crystals: From Self-Organized Nanostructures to Applications, Series: NanoScience and Technology*, Li, Q. (Ed.), Chapter 4, Springer-Verlag: Berlin, 101.
[12] Prasad, S. K., Sandhya, K. L., Nair, G. G., Hiremath, U. S., Yelamaggad, C. V., & Sampath, S. (2006). *Liq. Cryst.*, *33*, 1121.
[13] Pratibha, R., Park, K., Smalyukh, I. I., & Park, W. (2009). *Opt. Express*, *17*, 19459.
[14] Khatua, S., Manna, P., Chang, W. S., Tcherniak, A., Friedlander, E., Zubarev, E. R., & Link, S. (2010). *J. Phys. Chem.*, *114*, 7251.
[15] Milette, J., Toader, V., Reven, L., & Lennox, R. B. (2011). *J. Mater. Chem.*, *21*, 9043.
[16] Vardanyan, K. K., Walton, R. D., & Bubb, D. M. (2011). *Liq. Cryst.*, *38*, 1279.
[17] Pandey, A. S., Dhar, R., Kumar, S., & Dabrowski, R. (2011). *Liq. Cryst.*, *38*, 115.
[18] Vardanyan, K. K., Walton, R. D., Sita, D. M., Gurfinkiel, I. S., & Saidel, W. M. (2012). *Lig. Cryst.*, *39*, 595.
[19] Vardanyan, K. K., Sita, D. M., Walton, R. D., Saidel, W. M., & Jones, K. M. (2013). *RSC Adv.*, *3*, 259.
[20] Marino, L., Marino, S., Wang, D., Bruno, E., & Scaramuzza, N. (2014). *Soft Matter*, *10*, 3842.
[21] Hadjichristov, G. B., Marinov, Y. G., Petrov, A. G., Bruno, E., Marino, L., & Scaramuzza, N. (2014). *J. Appl. Phys.*, *115*, 083107.
[22] Pikin, S. A. (1991). *Structural Transformations in Liquid Crystals*, Gordon and Breach Science Publishers: New York.
[23] Hinov, H. P., Bivas, I, Mitov, M. D., Shoumarov, K., & Marinov, Y. (2003). *Liq. Cryst.*, *30*, 1293.
[24] Marinov, Y., Petrov, A. G., & Hinov, H. P. (2006). *Mol. Cryst.Liq. Cryst.*, *449*, 33.
[25] Kumar, P., & Krishnamurthy, K. S. (2007). *Liq. Cryst.*, *34*, 257.
[26] Buka, Á., Tóth-Katona, T., Krekhov, A., & Pesch, W. (2013). In: *Flexoelectricity in Liquid Crystals. Theory, Experiments and Applications,* Buka, Á., & Eber, N. (Eds.), Chapter 4, Imperial College Press: London, 101.
[27] Aguirre, L. E., Anoardo, E., Eber, N., & Buka, A. (2012). *Phys. Rev. E*, *85*, 041703.
[28] Hinov, H. P., Bivas, I, Mitov, M. D., & Shoumarov, K. (2003). *Liq. Cryst.*, 2003, *30*, 945.
[29] Li, F., Buchnev, O., Cheon, C. I., Glushchenko, A., Reshetnyak, V., Reznikov, Y., Sluckin, T. J., & West, J. L. (2006). *Phys. Rev. Lett.*, *97*, 147801.
[30] Li, F., Buchnev, O., Cheon, C. I., Glushchenko, A., Reshetnyak, V., Reznikov, Y., Sluckin, T. J., & West, J. L. (2007). *Phys. Rev. Lett.*, *99*, 219901.
[31] Chen, H. Y., & Lee, W. (2006). *Appl. Phys. Lett.*, *88*, 222105.
[32] Lee, C.W., & Shih, W.P. (2010). *Mat. Lett.*, *64*, 466.